Advances in Military Technology
Vol. 18, No. 2, 2023, pp. 179-194
ISSN 1802-2308, eISSN 2533-4123
DOI 10.3849/aimt.01800

Planing of the Finite Aspect Ratio Plate at Subsonic, Transonic and Supersonic Speeds

O. Mayboroda* and A. Derepa

Department of Navy, Institute of Armament and Military Equipment of Armed Forces of Ukraine, Kyiv, Ukraine

The manuscript was received on 17 January 2023 and was accepted after revision for publication as research paper on 27 October 2023.

Abstract:

The mechanics of underwater supercavitating projectiles are currently being extensively researched. The disadvantage of such projectiles is their movement instability. There is a proposal to use stern planing plates to stabilize projectile's movement. However, the hydrodynamic characteristics of planing plates are known only for low subsonic speeds. This article describes a load study on a planing plate at subsonic, transonic and supersonic speeds with detached and attached shock waves. The obtained calculation results of normal forces satisfactorily agree with the known theoretical solutions and experimental data and can be used to calculate the motion stabilization of supercavitating underwater projectiles with planing stern plates.

Keywords:

planing, supercavitating projectiles, supersonic speeds

1 Introduction

As it is known, one of the promising ways to improve the effectiveness of underwater weapons is the use of super-high speeds in the supercavitation mode. Some experiments on supercavitating projectiles, whose speeds were up to 1 300, 1 350 and 1 549 m/s, respectively, are known [1-3]. For comparison, underwater sonic speed is about 1 450 m/s. Under such speeds thermodynamic features of water as a compressible fluid appear and its flow is accompanied by known gas-dynamic effects – compression shocks, shock waves etc.

The disadvantages of supercavitating projectiles are a short range, which is limited by the capabilities of the power plant, and a fundamental uncontrollability due to

* *Corresponding author: Department of Navigation and Ships Control of the Water Transport Institute named after Hetman Petro Konashevych-Sahaidachny of the State University of Infrastructure and Technologies, 9 Kyrylivska str., Kyiv, UA-02000 Ukraine. Phone: +380 98 842 17 37, E-mail: olexander.mayboroda@gmail.com. ORCID 0000-0003-3919-8088.*

the lack of reliable hydroacoustic communication. The technical weakness of such projectiles is their own instability of movement, since the working point of a resistance force in the vicinity of the nose critical point excludes the appearance of hydrodynamic damping forces.

At the moment, the study of movement of supercavitating projectiles, taking into account the compressibility of the fluid, has been extensively developed. In [4-8], the results of research for supercavitating motion of ballistic projectiles in water at subsonic, transonic and supersonic speeds are presented. Some work is devoted to the search for supercavitating supersonic projectile water entrance [9, 10].

Many works are devoted to the study of controllability and manoeuvrability of high-speed underwater projectiles. In particular, the trajectory stability of high velocity water entry projectiles is examined experimentally in [11]. The inertia forces in the curvilinear movement of a supercavitating projectile in the vertical and horizontal planes were studied in [12, 13].

In some studies, possibilities of stabilizing the movement of projectiles are considered. As a kind of stable motion mode [14], the tail of the projectile can collide intermittently with the upper and lower surfaces of the cavity to provide a lifting force and restoring moment. In [15], by changing jet strength and model's length, a series of numerical simulations is studied on the interaction between ventilated cavity and supersonic tail jets which focused on the motion stabilization of supercavitating projectiles. In [16], the manoeuvring cavity model is applied to a supercavitating projectile at low subsonic speeds with planing force in the longitudinal plane. The planing force is produced to provide the restoring force and pitching moment for the stabilization of the movement.

It is of interest, according to example [16], to use the planing force to stabilize the motion of a supercavitating projectile both in the longitudinal and transverse planes at subsonic, transonic and supersonic speeds. For this purpose, it is possible to install a few stern plates which glide along a cavity surface and create hydrodynamic damping of the respective direction. In order to implement this damping method, it is necessary to know the loads on the planing plates at the appropriate speeds.

The purpose of this paper is to study the hydrodynamic loads of finite aspect ratio planing plates in a range of subsonic, transonic and supersonic speeds. Planing on the surface of incompressible water is investigated enough. As far as it is known, the gas-dynamic properties of the water have not yet been taken into consideration.

2 Purpose and Tasks of Research

The purpose of the research is to determine the hydrodynamic characteristics of the finite aspect ratio plates during high-speed planing for their possible use as stabilizers of the supercavitating projectile motion.

To achieve this purpose, the following tasks were solved:

- to determine the gas-dynamic properties of water as a compressible fluid,
- to establish the influence of the Mach number on the hydrodynamic characteristics of the planing plate at subsonic speeds,
- to investigate the formation processes of detached and attached shock waves in water,
- to analyse the interaction of shock waves with the free surface of the fluid,
- to establish the influence of the Mach number on the hydrodynamic characteristics of the planing profile at transonic and supersonic speeds,

- to investigate the hydrodynamic characteristics of finite aspect ratio plates during planing at transonic and supersonic speeds.

3 Gas-dynamic Properties of Water

The demonstration of water compression has several characteristics. In water, as a condensed medium, the molecules are short-distance and have a strong interaction. When such a medium is compressed, the internal pressure rises quickly, which, unlike gases, is not thermal, but elastic in nature. This determines the most important characteristics of the water behaviour during compression.

At pressures up to $p < 3 \times 10^9$ Pa the water state equation has the isentropic form Theta [17]

$$p = B(s)\left[\left(\frac{\rho}{\rho_0}\right)^k - 1\right] \tag{1}$$

where the entropy function $B(s)$ depends less on the initial entropy and can be accepted as $B = 2.987 \times 10^8$ Pa at the temperature T from 0 °C to 60 °C; ρ is the water density and ρ_0 is the water density extrapolated to zero pressure; k is the isentropic index which is equal to 7.15.

Pressure up to $p = 3 \times 10^9$ Pa corresponds to the Mach numbers below 1.5. To this range, all further evaluations of the hydrodynamic characteristics of the planing plate are concerned.

At $B = \text{const}$, the state Eq. (1) is reduced to the form $p = p(\upsilon)$, where υ is the water specific volume. Consequently, under the considered conditions, water is a barotropic medium, and its internal energy e is the sum of two functions, one of which depends only on the specific volume, and the other – only on the entropy s

$$e = e_1(\upsilon) + e_2(s) \tag{2}$$

Substituting Eq. (2) into the Gibbs relation, we get

$$\frac{\mathrm{d}e_1}{\mathrm{d}\upsilon}\mathrm{d}\upsilon + \frac{\mathrm{d}e_2}{\mathrm{d}s}\mathrm{d}s = T\mathrm{d}s - p\mathrm{d}\upsilon$$

where it comes from

$$T = T(s),\ s = s(T)$$

Thus, isentropic processes in water are isothermal.

The state Eq. (1) taking into account the given assumptions can be reduced to the form of Poisson's adiabatic

$$\frac{p+B}{\rho^k} = \frac{B}{\rho_0^k} = \text{const}$$

Then, as it is known, the Bernoulli equation for water will differ from that for gas by the addition of pressure

$$\frac{V^2}{2} + \frac{k}{k-1}\frac{p+B}{\rho} = \text{const}$$

where V is the velocity of water.

Accordingly, the expressions for the speed of sound a, analogous to the known gas-dynamic functions of density $\varepsilon(M)$ and pressure $\pi(M)$ in the case of water have the forms

$$a = \sqrt{\frac{k(p+B)}{\rho}} \tag{3}$$

$$\varepsilon(M) = \left(1 + \frac{k-1}{2} M^2\right)^{\frac{-1}{k-1}} \tag{4}$$

$$\pi(M) = \left(1 + \frac{k-1}{2} M^2\right)^{\frac{-k}{k-1}} \tag{5}$$

Figs 1 and 2 show graphs comparison of gas-dynamic functions of density (4) and pressure (5) for water and air in the range of Mach numbers $M \leq 1.5$.

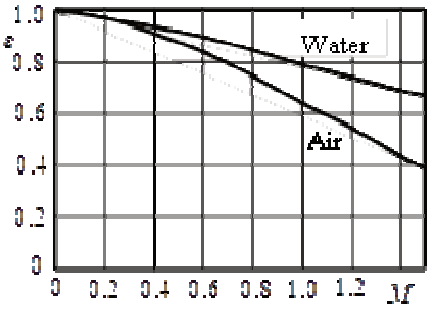

Fig. 1 Gas-dynamic functions of density for water and air

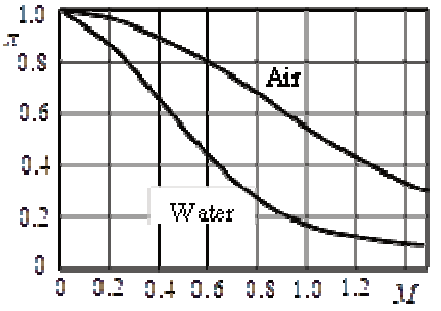

Fig. 2 Gas-dynamic functions of pressure for water and air

As we can see, the compressibility of water can be neglected only within $M \leq (0; 2)$, while for air it can be assumed to be $M = (0.25; 0.3)$. As number M increases, water noticeably exhibits greater elasticity than air (Fig. 1). The predominant value of constant internal pressure explains the significant drop in "thermal" pressure during isentropic expansion of water compared to air (Fig. 2).

4 Planing at Subsonic Speeds

4.1 Planing of Profile

The planing of the profile is shown in Fig. 3, where l_0 is the part of the profile length submerged relative to an undisturbed fluid surface, l is the profile wetted length, ψ is the trim angle, V is the speed of movement. The increase in the profile wetted length as compared with its length submerged relative to an undisturbed fluid surface reflects the effect of the bow backwater flow of fluid.

The depicted profile is a cross-section of the further considered plate with an aspect ratio of $\lambda \geq 0.01$ ($\lambda = 1/b$, where b is the plate width), during planing with a speed V and trim angles of $\psi \leq 60°$ at numbers $M \leq 1.5$.

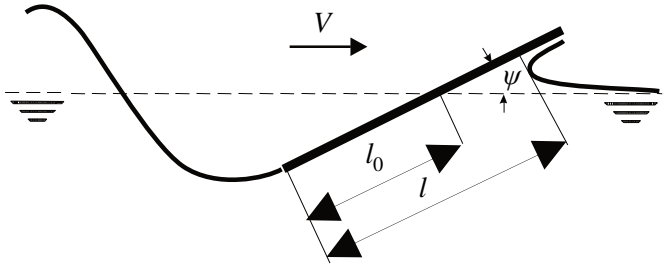

Fig. 3 Planing of a flat profile

In the Wagner analogy [18], a flow under the planing plate corresponds to that under the underside of a thin wing. For such a surface, experimental load data are available in a broad range of Mach numbers [19] and using the local linearization method, the effect of the Mach number on the load increase has been estimated [20].

A characteristic feature of the pressure distribution on the planing plate is the presence of only positive values of the pressure coefficient and a clearly expressed maximum at the critical point of flow braking. As shown by Kusukawa [21], the pressure distribution on the underside of a flat profile in the range $M \leq 1$ is affinity-like.

In aerodynamics, the approximate Prandtl-Glauert rule [17] is widely used, which establishes a dynamic similarity between the values of the pressure coefficient at the profile lower surface and the integral characteristics of its load when flowing around an incompressible fluid and a subsonic gas flow.

Let us estimate the value of the pressure coefficient at the profile critical point for different numbers M obtained by the Prandtl-Glauert rule and direct determination from the isentropic Eq. (5). In the first case, we have the value $\overline{p}_0 = 1/\sqrt{\left(1-M^2\right)}$, that is, the known similarity factor of the Prandtl-Glauert. In the second case, representing the pressure coefficient at the braking point in the form

$$\overline{p}_0 = \frac{(p_0 + B) - (p_\infty + B)}{\frac{\rho V^2}{2}} = \frac{2}{kM^2}\left(\frac{1}{\pi(M)} - 1\right)$$

we get the isentropic similarity factor

$$k_M = \frac{2}{kM^2}\left[\left(1 + \frac{k-1}{2}M^2\right)^{\frac{k}{k-1}} - 1\right] \tag{6}$$

Taking into account the affinity-like similarity of the pressure distribution on the profile lower side, it can be assumed that the value Eq. (6) can also be the similarity factor of the load integral characteristics of this surface for the modes $0.2 < M \leq 1$ of manifestation of the compressibility of fluid.

Fig. 4 shows the comparison of the similarity factor k_M Eq. (6) for water and air with the Prandtl-Glauert factor, as well as with experimental data on the change in the derivative of the normal force coefficient C_n^{ψ} on the profile lower surface in air [19] and the results of an approximate theoretical assessment of such an effect in water [20].

Satisfactory agreement of the given results allows us, for the indicated flow conditions, to recommend the similarity factor k_M Eq. (6) for taking into account the compressibility of various media at the Mach numbers $0.2 < M \leq 1$. In contrast to the Prandtl-Glauert rule, the similarity factor k_M takes into account the media thermodynamic properties and, as it is shown below, can be generalized to a supersonic regime with a detached shock wave.

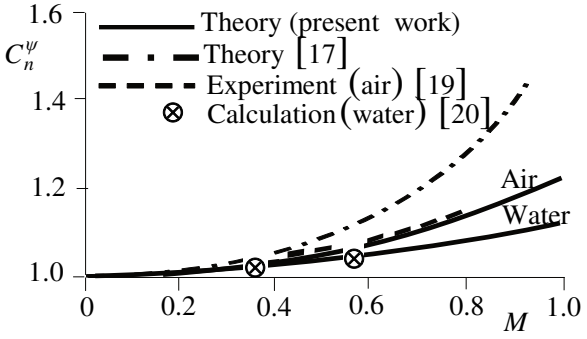

Fig. 4 Effect of the Mach number on the profile hydrodynamic load

4.2 Planing of the Finite Aspect Ratio Plate

The absence of nonlinear effects of finite-span wings during planing allows us to generalize the well-known theory of Young [19] to the case of a plate planing. The corresponding Young formula for the derivative of the normal force coefficient C_n^ψ of the finite aspect ratio plate during planing at subsonic speed has the form

$$C_n^\psi = \frac{\pi C_{n0}^\psi}{\pi + 2\lambda C_{n0}^\psi} \tag{7}$$

where C_{n0}^ψ is the derivative of normal force coefficient of the planing profile ($\lambda = 0$) at the corresponding number $M < 1$.

On a planing plate, the flow at the inner points of the surface remains subsonic at $M \leq 1$. In the same range of numbers M, expression Eq. (6) of the factor k_M which considers the influence of fluid compressibility is valid. So at small trim angles ψ we have

$$C_{n0}^\psi = \frac{2\pi}{kM^2}\left[\left(1 + \frac{k-1}{2}M^2\right)^{\frac{k}{k-1}} - 1\right] \quad M \leq 1 \tag{8}$$

Based on the assumption of an affine-like distribution of pressure coefficients with increasing number M, it is possible to obtain the derivative of the normal force coefficient of the finite aspect ratio plate during planing at $M \leq 1$ and $\psi \leq 60°$ in the form

$$C_n^{\psi} = \frac{\pi}{\dfrac{1}{k_{\psi} k_{\mathrm{M}}} + 2\lambda} \quad M \leq 1 \quad \psi \leq 60^{\circ} \quad \lambda \leq 0.01 \tag{9}$$

where k_{ψ} is the coefficient taking into account the trim angle according to Sedov's nonlinear theory [22].

Let us consider the effect of compressibility on the value of the bow backwater flow of a fluid during the subsonic planing of a finite aspect ratio plate. In the linear approximation, the subsonic vortex-free flow of a compressible fluid is potential. Therefore, in the well-known Wagner model [18], a modified expression can be used for the velocity potential at the impact of a plate in a compressible fluid, which differs from the potential of a similar flow of an incompressible fluid by the factor of the Prandtl-Glauert.

After solving Wagner's integral immersion equation, generalized in the above way for the case of subsonic motion of a compressible fluid, an expression of the relative bow backwater flow during planing can be obtained

$$\frac{l}{l_0} = \frac{1}{\sqrt{1-M^2}} \left(\frac{l}{l_0}\bigg|_{M=0} + 1 \right) - 1 \quad M < 1 \tag{10}$$

In the wing theory, the Prandtl-Glauert method is considered valid up to the critical value of the number M. At the planing of a flat plate, the critical value of the number M is equal to 1. So the physical incorrectness of expression (10) at $M = 1$ is obvious. It can be assumed that the replacement in Eq. (10) of the Prandtl-Glauert factor by the value k_{M} Eq. (6), which was successfully used above in determining the load (Fig. 4), will be justified in this case as well. So, the expression for the relative value of the bow backwater flow at numbers $M \leq 1$ has the form

$$\frac{l}{l_0} = \frac{3 + \sqrt{1 + \dfrac{1}{\lambda_0}}}{kM^2} \left[\left(1 + \frac{k-1}{2} M^2 \right)^{\frac{k}{k-1}} - 1 \right] - 1 \quad M \leq 1 \tag{11}$$

The affinity-like nature of the pressure coefficient distribution with increasing number M allows us to assume the preservation of the relative position of the pressure centre. Since the longitudinal moment is zero at zero normal force on the planing plate, the focus along the trim angle coincides with the pressure centre.

The coefficient of pressure resistance of the planing plate at $M \leq 1$ is determined according to the well-known definition

$$C_{xp} = C_n^{\psi} \psi \sin \psi \tag{12}$$

where C_n^{ψ} is taken in accordance with Eq. (9), and the coefficient of friction resistance can be estimated by the Prandtl-Schlichting formula with correction for compressibility [19].

5 Planing at Transonic and Supersonic Speeds

5.1 Features of Supersonic Planing

When a plate moves with supersonic speed, a shock wave moves ahead of it. The isentropic character of the water state equation makes it possible to consider a formation and propagation of this shock wave in the quasi-acoustic approximation. Accordingly, it is possible to use the known conditions of dynamic compatibility [23] and the basic relationships that differ from those known for gas only by adding the value B to the pressure. Instead, an additional complication is the need to take into account the free boundary of the fluid.

At the point of intersection of the shock wave front with the free surface, the centred Prandtl-Meier rarefaction wave departs, and the flow turns in the direction of the free surface [24]. Such a problem has an automodel solution only for a sufficiently weak shock wave, behind which the fluid velocity is sonic or supersonic [23].

As far as it is known, the solution of the problem of the supersonic flow of a finite dimensions body with a fluid with a free surface has not yet been obtained. In any case, the formulation of such problems should include the choice of a possible configuration of shock waves, whether the shocks belong to strong or weak types, as well as the criterion for the steady flow existence. The accuracy of the choice of one or the other option is finally determined by the correspondence between the solution obtained and the actual flow view and the results of the experiment.

Let us consider the implementation of the above conditions for the uniqueness of the solution in relation to the considered problem of supersonic planing. Given the complexity of the problem, let's first analyse a simplified case – planing of a flat profile, that is, an infinite aspect ratio plate.

Since there is no further pressure increase on the flat profile after the shock wave, it is possible to accept this shock wave as belonging to a weak type. Taking into account the absence of mixed flow around the plate and the associated instability, we assume the existence of a quasi-stationary solution to the problem.

Let us consider sequentially the regimes of supersonic flow around a planing plate. At $M = 1$ a detached direct shock wave is formed in front of the plate. Subsequently, with an increase in the flow velocity at M', the shock attaches to the plate, becomes curvilinear, and the flow behind the shock deviates by the trim angle of the plate. At M'', the flow behind the shock becomes supersonic.

As shown in the series of works on supersonic gas jets [25], the estimation of the limiting flow rotation angles in the attached shock wave and of flows with a free boundary is preserved. Based on these assumptions, an approximate calculation of the flow rotation angles and the incline shock wave angles in water at $M \leq 1.5$ was performed.

Fig. 5 shows the flow rotation angles α of the water in the shock wave with the shock inclination angle β at different numbers M. Additionally, the corresponding dependences for air, emphasizing the exceptionally low compressibility of water, are shown. Fig. 6 shows the dependence of the number M', at which the shock wave attaches the profile with increasing speed, on the trim angle ψ.

As it can be seen, the planing profile at trim angles ψ more than or equal to 2.8° for the Mach numbers below 1.5 is always streamlined with a detached shock wave.

The similar limit angle for air is equal to 12°, which also indicates a lower compressibility of water.

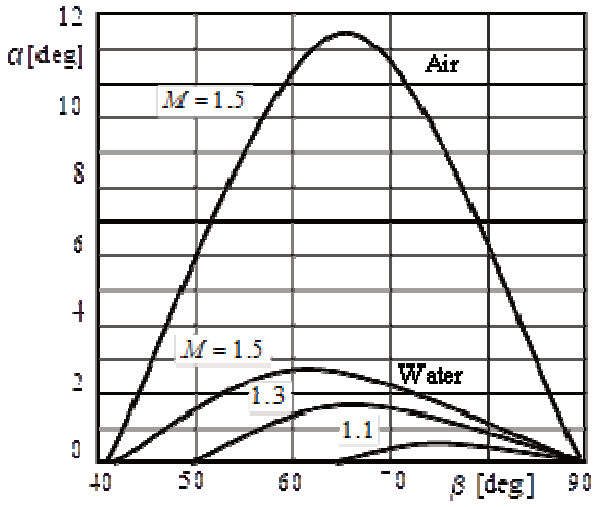

Fig. 5 Dependences of flow rotation angle of water and air in shock wave on shock inclination angle

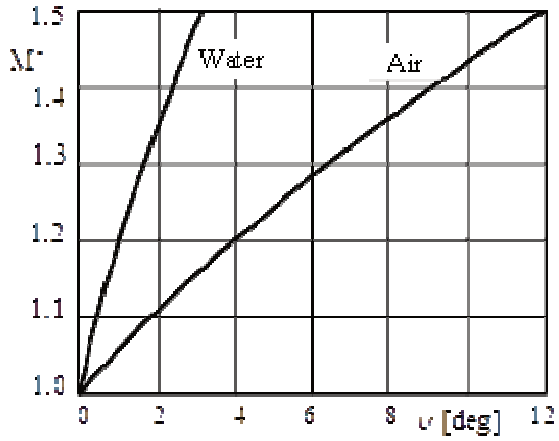

Fig. 6 Dependences of number M' of shock wave attachment in water and air on profile trim angle

Fig. 7 shows a comparison of the recovery factors of the total pressure in the detached shock wave for water and air, calculated according to the well-known representation [23]

$$\chi = \frac{p_{02}}{p_{01}} = \left(\frac{k+1}{k}\right)^{\frac{k+1}{k-1}} \frac{M_1^{\frac{2k}{k-1}}}{\left(1+\frac{k-1}{2}M_1^2\right)^{\frac{k}{k-1}} \left(kM_1^2 - \frac{k-1}{2}\right)^{\frac{1}{k-1}}}$$

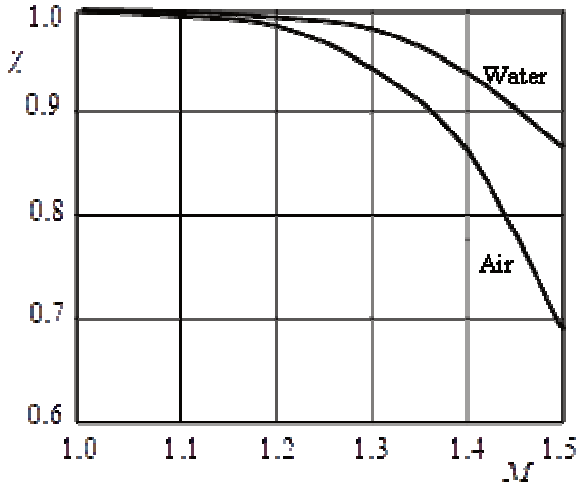

Fig. 7 Total pressure recovery factor in detached shock wave for water and air

As it can be seen, shock waves in water are relatively less strong, which justifies the admissibility of the quasi-acoustic approximation in the analysis of processes of their formation, in particular near the free surface of the fluid.

Similar laws are of great importance in applications of the theory of compressible fluid flows. In particular, the thermodynamic properties of the environment are taken into account by the fundamental thermodynamic parameter [23]

$$\Gamma = \frac{a^4}{v^3}\frac{\partial^2 v}{\partial p^2}\bigg|_s - 1 \tag{13}$$

where a is the sound speed; v is the specific volume, and the derivative is taken at constant entropy. For a perfect gas, the parameter Γ is constant and equal to the gas adiabatic index.

For water, value k in the Theta Eq. (1) formally has the meaning of an adiabatic index, but is not a ratio of heat capacities. However, by directly differentiating the state Eq. (1) and substituting expression (4) for the water sound speed into Eq. (13), it can be shown that for water at $p < 3 \times 10^9$ Pa the parameter Γ is also constant and is equal to k.

Therefore, for water within the limits of the Theta equation validity, the similarity laws of the perfect gas dynamics can be applied when the gas adiabatic index is substituted by value k. In particular, an approximate estimate of the shock wave attachment mode in water, shown in Fig. 6, according to the value of the Karman-Chen similarity criterion, satisfactorily agrees with the solution of a similar problem for gas obtained by Vincenti and Wagoner [26] using the hodograph method.

5.2 Planing Profile with Detached Shock Wave

The detached shock wave C (Fig. 8) interacts with the fluid free surface A. Supersonic flow in the convex head part of the shock turns into subsonic. The remaining part of the shock decomposes into a weak discontinuity and the flow behind it remains supersonic. From a free surface, the shock is reflected by the centred Prandtl-Meyer

expansion wave *PM*. The free surface de-formation is determined by the distance from the shock to the profile, the so-called thickness of the shock layer.

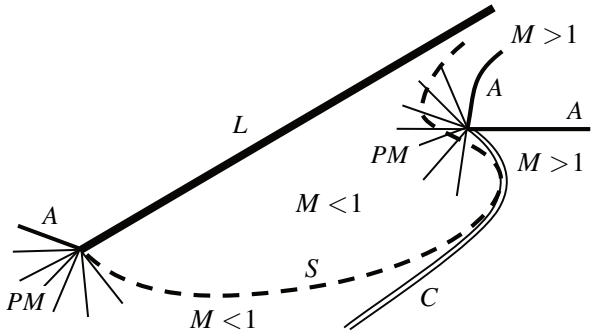

Fig. 8 Planing profile with detached shock wave

The subsonic area of the flow around the profile is separated from the main supersonic flow by the contact discontinuity line *S* and the centred stern Prandtl-Meyer rarefaction wave.

With a small shock layer thickness (the number *M* is close to value M') at the point of the shock wave reflection, the free surface of the fluid is sharply curved [25], forming a spray jet. With a greater shock layer thickness, the free surface perturbation is insignificant (a case close to self-similar) and can be neglected [27].

When evaluating the profile load, let us assume that the subsonic flow on the profile conditionally has a speed at infinity with number *M* after the direct shock wave. This not entirely strict assumption, known as the correspondence principle, is approximately fulfilled for a sufficiently large shock layer thickness and for the absence of supersonic zones on the streamlined body [27]. Therefore, with sufficient accuracy for engineering applications, it is possible to obtain an expression for the similarity factor k_M from the Rayleigh formula, which shows the relative change in the normal force coefficient of the planing profile on the effect of number *M* for trim angles $\psi > 2.8°$

$$k_M = \frac{2}{kM^2}\left[\frac{\left(\frac{k+1}{2}M^2\right)^{\frac{k}{k-1}}}{\left(\frac{2kM^2}{k+1}-\frac{k-1}{k+1}\right)^{\frac{1}{k-1}}}-1\right] \quad 1<M<M' \tag{14}$$

5.3 Planing Profile with Attached Shock Wave

The shock attaches to the profile at M', and the flow around the profile becomes supersonic at M''. Behind the attached shock, the nasal critical point on the profile disappears [28] and the flow around the planing profile becomes similar to that of a thin symmetrical wedge.

Therefore, we can use the well-known expression to calculate the derivative of the normal force coefficient C_n^{ψ} of a profile during supersonic planing

$$C_n^{\psi} = \frac{4}{\psi(k+1)}\left(\sin^2\beta - \frac{1}{M^2}\right) \quad M' \le M \le 1.5 \tag{15}$$

where the inclination angle β of the shock wave is determined by known way [23].

In Fig. 9 in the criteria of transonic similarity C_n^{ψ} and $\overline{M}$ [23], the calculation results of load on the planing profile at small trim angles in the range $0.95 \le M \le 1.25$ are compared with the results of Nishiyama and Omar [20], Vincenti and Wagoner [26], Yoshihara [29] and Guderley [30]. Here, values M' and M'' correspond to values $\overline{M} = 1.18$ and $\overline{M} = 1.26$. Value $M = 1$ corresponds to value $\overline{M} = 0$.

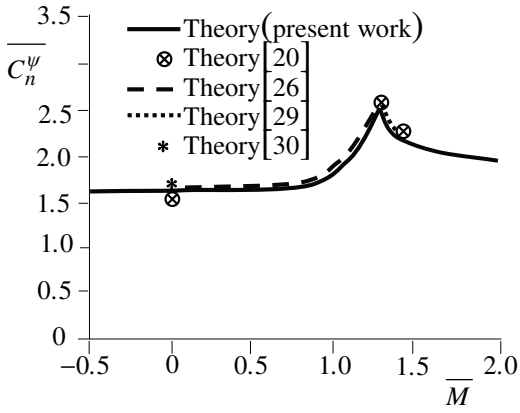

Fig. 9 Hydrodynamic characteristics profile during transonic planing with small trim angles

Vincenti and Wagoner [26] investigated numerically the flow around a thin wedge with a detached shock wave at $0 < \overline{M} < 1.05$. Yoshihara [29] obtained an approximate solution of the hodograph equation for the flow around a thin wedge in the range of regimes $1.18 \le \overline{M} \le 1.26$.

In the range of $1.05 \le \overline{M} \le 1.18$, Fig. 9 shows the interpolated values. Since in the linear theory of supersonic flow it is assumed that the load is distributed equally between the lower and upper parts of the profile, the results of works [26] and [29] are shown in Fig. 9 for half the calculated wedge load.

Shown in Fig. 9, the calculated values $\overline{C_n^{\psi}}$ for the supersonic flow behind the attached shock wave at $\overline{M} > 1.26$ satisfactorily correspond with those given in Guderley's monograph [27]. Guderley's result [30] of the flow around the lower surface of the plate at $M = 1$ is shown on Fig. 9 as a point.

As it can be seen in Fig. 9, the obtained calculated estimates for the load of a flat profile during planing at $M \le 1.5$ agree satisfactorily with known theoretical results and can be used to calculate the hydrodynamic characteristics of a planing plate.

At $M \ge M''$ the pressure centre of the planing profile is located in the middle of the wetted length.

5.4 Planing the Plate with Finite Aspect Ratio

Let us determine the value of the relative bow backwater flow during the supersonic planing of a finite aspect ratio plate. The flow behind a detached shock wave in water

in the hydroacoustic approximation is isentropic and therefore potential. Therefore, the relative bow backwater in the subsonic flow behind the detached shock wave can be estimated with the replacement of the Prandtl-Glauert coefficient in Eq. (10) by value k_M Eq. (14)

$$\frac{l}{l_0}=\frac{3+\sqrt{1+\dfrac{1}{\lambda_0}}}{k_M^2}\left[\frac{\left(\dfrac{k+1}{2}M^2\right)^{\frac{k}{k-1}}}{\left(\dfrac{2k_M^2}{k+1}-\dfrac{k-1}{k+1}\right)^{\frac{1}{k-1}}}-1\right] \quad 1\le M<M' \tag{16}$$

Expression (16) is sufficiently valid at trim angles of 2.8°.

In the case of supersonic flow of an ideal fluid behind the attached shock wave on the planing profile, there is no critical braking point [28] and, therefore, there is no bow backwater flow of the fluid.

Accounting the finite aspect ratio effect on the hydrodynamic load of the planing plate during supersonic moving with a detached shock wave can be performed according to the generalized Young formula (7), and with an attached shock wave – according to Hilton's method [19].

For the accepted assumptions, it can be assumed that the influence of the plate aspect ratio on the pressure centre location in the range of modes $0<M<M''$ can be approximately estimated by the methods adopted for an incompressible fluid, and at modes $M\ge M''$ the centre of pressure is located at the wetted length middle.

Figs 10 and 11 show the hydrodynamic characteristics of the planing plate with different initial aspect ratio and trim angles in the range of $0\le M\le 1.5$. Fig. 10 shows modes with the attached shock wave, and Fig. 11 – with the detached shock wave. Values C_n^{ψ} at $M=0$ in Figs 10 and 11 correspond to the known results in planing over the incompressible fluid surface.

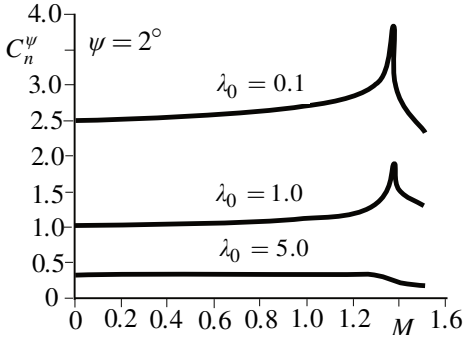

Fig. 10 Hydrodynamic loads on plates at planing with attached shock wave

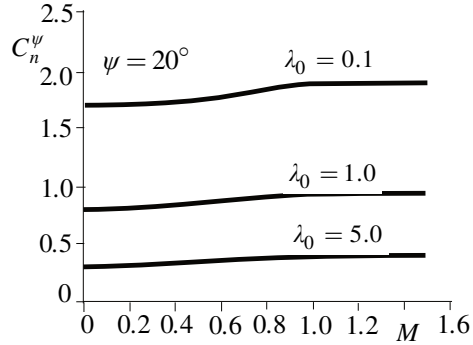

Fig. 11 Hydrodynamic loads on plates at planing with detached shock wave

6 Conclusion

In this article, the gas-dynamic properties of water in the Mach number range up to 1.5 were studied. The obtained data establish the effect of water compressibility on the hydrodynamic characteristics of the planing profile and plate in the given speed range.

The isentropic similarity index of pressure coefficients of incompressible fluid flowing along the profile bottom surface to their values for Mach numbers up to 1.5 is proposed. Unlike the Prandtl-Glauert rule, the proposed approach takes into account the thermodynamic properties of the medium.

The formation processes of attached and detached shock waves in water are considered. A physical model of the supersonic motion of a planing plate has been constructed. The interaction of detached and attached shock wave with the free water surface is considered.

A quantitative assessment of the hydrodynamic characteristics of finite aspect ratio plates during planing at Mach numbers up to 1.5 with detached and attached shock wave is proposed. The obtained results agree satisfactorily with the known theoretical solutions and experimental data and can be used to calculate the hydrodynamic stabilization of the motion of supercavitating underwater projectiles with planing stern plates.

References

[1] SAVCHENKO, Yu.N. Experimental Investigation of Supercavitating Motion of Bodies. In: *Supercavitating Flows.* Belgium: Defence Technical Information Centre, 2001, pp. 1-24.

[2] VLASENKO, Yu.D. Experimental Investigations of Supercavitation Flow Regimes at Subsonic and Transonic Speeds. In: *Proceedings of 5th International Symposium on Cavitation.* Osaka, 2003.

[3] KIRSCHNER, I.N. Results of Selected Experiments Involving Supercavitating Flows. In: *Supercavitating Flows*. Brussels: NATO, 2001.

[4] SEREBRYAKOV, V.V., I.N. KIRSCHNER and G.H. SCHNERR. High Speed Motion in Water with Supercavitation for Sub-, Trans-, Supersonic Mach Numbers. In: *Proceedings of 7th International Symposium on Cavitation.* Michigan: University of Michigan, 2009.

[5] ZHANG, Z., Q. MENG, Z. DING and J. GU. Effect of Compressibility on Supercavitating Flow around Slender Conical Body Moving at Subsonic and Supersonic Speed. *Ocean Engineering*, 2015, **109**, pp. 489-494. DOI 10.1016/ j.oceaneng.2015.09.027.

[6] WANG, C., G. WANG, M. ZHANG, B. HUANG and D. GAO. Numerical Simulation of Ultra-High Speed Supercavitating Flows Considering the Effects of the Water Compressibility. *Ocean Engineering*, 2017, **142**, pp. 532-540. DOI 10.1016/J.oceaneng.2017.07.041.

[7] DU, Y., C. WANG and Y. ZHOU. A Study on Supercavitation in Axisymmetric Subsonic Liquid Flow past a Slender Conical Body. *European Journal of Mechanics – B/Fluids*, 2018, **72**, pp. 264-274. DOI 10.1016/j.euromechflu. 2018.06.004.

[8] LI, D., B. HUANG, M. ZHANG, G. WANG and T. LIANG. Numerical and Theoretical Investigation of the High-Speed Compressible Supercavitating Flows. *Ocean Engineering*, **156**, pp. 446-455. DOI 10.1016/ j.oceaneng.2018.03.032.

[9] CHEN, C., T. SUN, Y. WEI and C. WANG. Computational Analysis of Compressibility Effects on Cavity Dynamics in High-Speed Water-Entry.

International Journal of Naval Architecture and Ocean Engineering, 2019, **11**(1), pp. 495-509. DOI 10.1016/J.IJNAOE.2018.09.004.

[10] JIANG, Y., Y. LI, J. GUO, L. YANG and H. WANG. Numerical Simulations of Series and Parallel Water Entry of Supersonic Projectiles in Compressible Flow. *Ocean Engineering*, 2021, **235**, 109155. DOI 10.1016/ J.OCEANENG.2021.109155.

[11] CHEN, T., W. HUANG, W. ZHANG, Y. QI and Z. GUO. Experimental Investigation on Trajectory Stability of High-Speed Water Entry Projectiles. *Ocean Engineering*, 2019, **175**, pp. 16-24. DOI 10.1016/ J.OCEANENG.2019.02.021.

[12] YU, K., W. ZOU, R.E. ARNDT and Z. GUANG. Supercavity Motion with Inertial Force in the Vertical Plane. *Journal of Hydrodynamics*, 2012, **24**(5), pp. 752-759. DOI 10.1016/S1001-6058 (11)60300-4.

[13] WANG, Z., K. YU, R.E.A. ARNDT, and Z. GUANG. Modelling and Simulation of Supercavity with Inertial Force in the Horizontal Curvilinear Motion. *China Ocean Engineering*, 2014, **28**, pp. 31-42. DOI 10.1007/S13344-014-0002-Y.

[14] WANG, Z. and H. LIU. Modelling and Simulations of the Supercavitating Vehicle with Its Tail-Slaps. *Journal of Fluids Engineering*, 2015, **137**(4), 041302. DOI 10.1115/1.4029330.

[15] ZHAO, X., M. XIANG, W. ZHANG, B. LIU and S. LI. Numerical Study on the Stability and Closure Position of Ventilated Cavity with a Supersonic Tail Jet. *Chinese Journal of Theoretical and Applied Mechanics*, 2021, **53**(12), pp. 3298-3309. DOI 10.6052/0459-1879-21-346.

[16] WANG, Z., K YU and R.E. ARNDT. A. Modelling and Simulations of Supercavitating Vehicle with Planing Force in the Longitudinal Plane. *Applied Mathematical Modelling*, 2015, **39**(19), pp. 6008-6020. DOI 10.1016/ J.APM.2015.01. 040.

[17] COLE, R.H. *Underwater Explosions.* New York: Dover Publications, 1965. ISBN 0-486-61384-4.

[18] WAGNER, H. About Processes of Impact and Planing on the Fluid Surface (in Germany). *Zeitschrift für Angewandte Mathematik und Mechanik*, 1932, **12**(4), pp. 193-213.

[19] HILTON, W.F. *High-Speed Aerodynamics*. London: Longmans, 1951. ISBN 1-124-04572-4.

[20] TETSUO, N. and F. KHAN. Compressibility Effects on Cavitation in High Speed Liquid Flow. II Transonic and Supersonic Liquid Flows. *Bulletin of the Japan Society of Mechanical Engineers,* 1981, **24**, pp. 655-661. DOI 10.1299/JSME1958.24.655.

[21] KUSUKAWA, K-I. On the Two-dimensional Compressible Flow over a Thin Symmetric Obstacle with Sharp Shoulders Placed in an Unbounded Fluid and in a Choked Wind Tunnel. *Journal of the Physical Society of Japan*, 1957, **12**, pp. 1031-1041. DOI 10.1143/JPSJ.12.1031.

[22] SEDOV, L.I. *Two-dimensional Problems in Hydrodynamics and Aerodynamics*. New York: Wiley, 1965. ISBN 0-470-77110-0.

[23] CHERNY, G.G. *Gas Dynamics* (in Russian). Moscow: Nauka, 1988. ISBN 978-5-02-013814-8.

[24] GRIB, A.A., O.S. RYSHOV and S.A. HRISTIANOVICH. The Theory of Short Waves (in Russian). *Journal of Applied Mechanics and Technical Physics*, 1961, pp. 63-75. ISSN: 0869-5032.

[25] *Supersonic Gas Jets* (in Russian). Novosibirsk: Nauka, 1983.

[26] VINCENTI, W.G. and C.B. WAGONER. *Transonic Flow past a Wedge Profile with Detached Bow Wave: General Analytical Method and Final Calculated Results.* [Technical Note]. Washington: NACA, 1951.

[27] GUDERLEY, K.G. *The Theory of Near-Sonic Flows* (in German). Berlin: Springer, 1957. ISBN 3-540-02152-3.

[28] NEILAND, V.J. To the Asymptotic Theory of Addition of a Supersonic Flow (in Russian). In: *Proceedings of the Russian Central Aerohydrodynamic Institute*. Moscow: TsAGI, 1975, pp. 3-16.

[29] YOSHIHARA, H. On the Flow over a Wedge in the Upper Transonic Region. In: *Proceedings of the Second US National Congress of Applied Mechanics.* Michigan: University of Michigan, 1954.

[30] GUDERLEY, K. The Flow over a Flat Plate with a Small Angle Attack at Mach Number 1. *Journal of the Aeronautical Science,* 1954, **21**(4), pp. 261-270. DOI 10.2514/8.2990.